The EMBO Journal (2009), 1–14 | © 2009 European Molecular Biology Organization | All Rights Reserved 0261-4189/09
www.embojournal.org

THE EMBO JOURNAL

Assembly of a β_2-adrenergic receptor—GluR1 signalling complex for localized cAMP signalling

Mei-ling A Joiner[1], Marie-France Lisé[2], Eunice Y Yuen[3], Angel YF Kam[4], Mingxu Zhang[1], Duane D Hall[1], Zulfiqar A Malik[1], Hai Qian[1], Yucui Chen[1], Jason D Ulrich[1], Alain C Burette[5], Richard J Weinberg[5], Ping-Yee Law[4], Alaa El-Husseini[2,*], Zhen Yan[3] and Johannes W Hell[1,*]

[1]Department of Pharmacology, University of Iowa, Iowa City, IA, USA, [2]Department of Psychiatry and Brain Research Center, University of British Columbia, Vancouver, British Columbia, Canada, [3]Department of Physiology and Biophysics, State University of New York, Buffalo, NY, USA, [4]Department of Pharmacology, University of Minnesota, Minneapolis, MN, USA and [5]Department of Cell and Developmental Biology, and Neuroscience Center, University of North Carolina, Chapel Hill, NC, USA

Central noradrenergic signalling mediates arousal and facilitates learning through unknown molecular mechanisms. Here, we show that the β_2-adrenergic receptor (β_2AR), the trimeric G_s protein, adenylyl cyclase, and PKA form a signalling complex with the AMPA-type glutamate receptor subunit GluR1, which is linked to the β_2AR through stargazin and PSD-95 and their homologues. Only GluR1 associated with the β_2AR is phosphorylated by PKA on β_2AR stimulation. Peptides that interfere with the β_2AR–GluR1 association prevent this phosphorylation of GluR1. This phosphorylation increases GluR1 surface expression at postsynaptic sites and amplitudes of EPSCs and mEPSCs in prefrontal cortex slices. Assembly of all proteins involved in the classic β_2AR–cAMP cascade into a supramolecular signalling complex and thus allows highly localized and selective regulation of one of its major target proteins.

The EMBO Journal advance online publication, 26 November 2009; doi:10.1038/emboj.2009.344
Subject Categories: signal transduction; neuroscience
Keywords: adrenergic; AMPA; localized; signalling

Introduction

Although cAMP can in general freely diffuse, it can also be spatially restricted and exert highly localized actions (e.g. Levitzki, 1988; Neubig, 1994; Zaccolo and Pozzan, 2002; Rebois and Hebert, 2003; Fischmeister *et al*, 2006; Richter *et al*, 2008; Dai *et al*, 2009). Evidence for constitutive association of G protein-coupled receptors and their downstream effectors, the trimeric G_s protein and adenylyl cyclase, with each other has been established and interactions of such complexes with downstream targets have been proposed to form the basis for spatially restricted cAMP signalling (Levitzki, 1988; Neubig, 1994; Rebois and Hebert, 2003; Dai *et al*, 2009). Here, we describe a complex containing the β_2-adrenergic receptor (β_2AR), G_s, adenylyl cyclase, PKA, and the AMPA receptor (AMPAR) GluR1 subunit that allows highly localized signalling by cAMP in neurons.

A brief period of high activity can permanently enhance synaptic transmission between neurons in the hippocampus. This long-term potentiation (LTP) has been a focus of intense study, as a tractable experimental model for learning and memory. Current evidence implicates trafficking of AMPARs to the postsynaptic membrane as the primary mechanism of LTP expression. AMPARs are tetramers formed by GluR1-4 subunits, with GluR1/2 and GluR2/3 heterotetramers accounting for the majority of AMPARs in the hippocampus (Hollmann and Heinemann, 1994; Wenthold *et al*, 1996; Dingledine *et al*, 1999) and GluR1/2 constituting the functionally by far prevailing AMPAR component at postsynaptic sites under basal conditions (Lu *et al*, 2009). The GluR1 subunit is thought to have a special function in initiating the remodelling associated with increased synaptic expression of AMPARs on LTP. Phosphorylation of GluR1 by PKA on serine 845 (S845) is critical for activity-driven accumulation of GluR1 at postsynaptic sites (Esteban *et al*, 2003) and fosters surface expression of GluR1 (Ehlers, 2000; Swayze *et al*, 2004; Sun *et al*, 2005; Oh *et al*, 2006; Man *et al*, 2007). Moreover, GluR1 is physically associated with PKA and the counteracting phosphatase calcineurin/PP2B, optimizing the efficacy of this regulation (Colledge *et al*, 2000; Tavalin *et al*, 2002).

Norepinephrine, released by an extensive network of fibres originating from the locus coeruleus, supports arousal and learning under novel and emotionally charged situations (Cahill *et al*, 1994; Nielson and Jensen, 1994; Berman and Dudai, 2001; Strange *et al*, 2003; Strange and Dolan, 2004; Minzenberg *et al*, 2008) and facilitates various forms of LTP in the dentate gyrus and CA1 region of the hippocampus (Thomas *et al*, 1996; Lin *et al*, 2003; Walling and Harley, 2004; Gelinas and Nguyen, 2005). However, the molecular basis of these noradrenergic actions is unclear. Norepinephrine acts through αAR and βAR. Stimulation of the β_1AR and β_2AR activates G_s, adenylyl cyclase, and PKA. The β_2AR is concentrated at excitatory postsynaptic sites in pyramidal neurons (Davare *et al*, 2001). We now show that GluR1 forms a signalling complex with the β_2AR, G_s, and adenylyl cyclase for highly localized GluR1 phosphorylation, which promotes surface expression of GluR1 and increases EPSC and mEPSC amplitudes in cortex.

Results

β_2AR and GluR1 colocalize in hippocampal neurons

Double labelling for the β_2AR and GluR1 in tissue slices from adult hippocampus showed prominent colocalization of

*Corresponding author: Department of Pharmacology, University of California, Davis, CA 95616-8636, USA. Tel.: +1 319 384 4732; Fax: +1 319 335 8930; E-mail: jwhell@ucdavis.edu
*Deceased.

Received: 21 January 2009; accepted: 27 October 2009

immunoreactive puncta (Figure 1A). Most of these puncta were closely associated with puncta immunoreactive for the presynaptic marker synaptophysin, suggesting that they represent bona fide synapses. Quantitative analysis indicates that >90% of the β_2AR puncta associated with synaptophysin were also positive for GluR1 (Figure 1B). Furthermore, >80% of GluR1 puncta associated with synaptophysin were also immunoreactive for β_2AR, implying that the large majority of GluR1-containing synapses also possess the β_2AR.

The precise localization of the β_2AR was determined by post-embedding immunogold labelling in the prefrontal cortex (PFC), which receives especially prominent noradrenergic innervation (e.g. Minzenberg *et al*, 2008). A large fraction of gold label was synaptic, and a large fraction of asymmetric axospinous synapses were immunopositive (Figure 1C). Gold particles concentrated over the postsynaptic density close to the postsynaptic membrane. Particles could also be seen within spines, in large dendritic shafts, in which they were typically associated with microtubules and in the cytoplasm of neuronal somata (data not shown).

After solubilization with Triton X-100 and removal of non-solubilized material by ultracentrifugation, immunoprecipitation of the β_2AR from rat forebrain (Figure 1D) led to co-immunoprecipitation of GluR1 (Figure 1E). This co-precipitation was specific, as the NMDA-type glutamate receptor (NMDAR) subunit NR2B, which has an overall structure and cellular distribution similar to GluR1, did not co-precipitate with the β_2AR, and control IgG did not immunoprecipitate GluR1 or the β_2AR. In contrast, immunoprecipitation of the NMDAR–PSD-95 complex (Leonard *et al*, 1998; Valtschanoff *et al*, 2000; Lim *et al*, 2002, 2003) did not result in co-precipitation of the β_2AR (Figure 1F). We conclude that the β_2AR assembles with GluR1-containing AMPARs, but not with NMDAR into a molecular complex at synapses.

GluR1 interacts with the β_2AR through PSD-95 and stargazin/γ2

PSD-95 co-immunoprecipitated with the β_2AR from rat brain extracts (Figure 2A). *In vitro* pull-down experiments indicate that this association is mediated by the C-terminus of the β_2AR. The distal end of the β_2AR C-terminus (DSPL), which conforms to a type 1 PDZ domain ligand, binds to the third PDZ domain of PSD-95 (Figure 2B). Stargazin (or γ2) and its homologues γ3, γ4, γ5, γ7, and γ8 (TARPs) associate with AMPARs to promote their surface expression and modulate their biophysical properties. Stargazin binds with its C-terminus to the first two PDZ domains of PSD-95, and this interaction is required for surface expression and postsynaptic

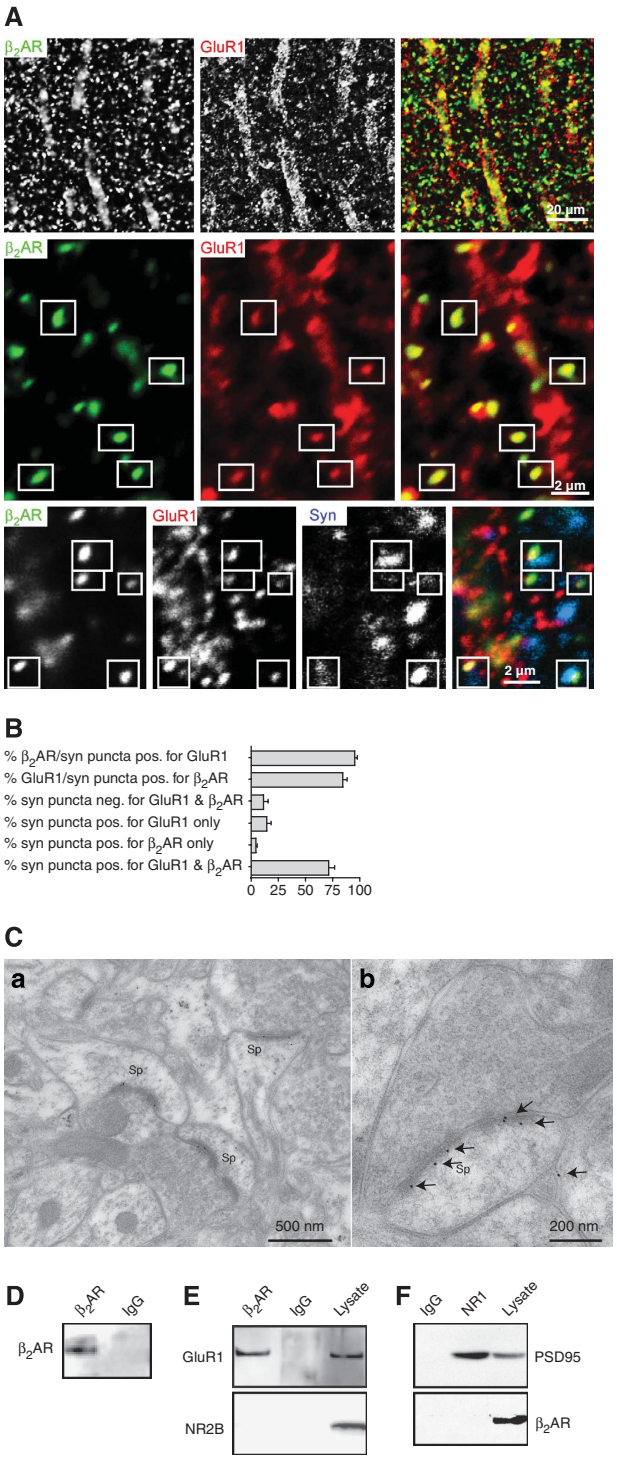

Figure 1 Colocalization and co-immunoprecipitation of β_2AR and GluR1. (**A**) Rat brain sections were triple-labelled for β_2AR (left panels; green in overlays), GluR1 (centre panels; red), and synaptophysin (blue in bottom right panel). GluR1 and β_2AR puncta colocalize with each other (boxes) and associate with synaptophysin puncta (triple overlay, bottom right panel) in the stratum radiatum of the CA1 area. (**B**) Quantification of the number of β_2AR, GluR1, or synaptophysin (syn)-labelled puncta that shows positive (pos.) or no (neg.) staining for one or both of the other proteins. More than 90% of puncta that are positive for the β_2AR and associated with synaptophysin are also positive for GluR1 (top bar) and >80% of puncta that are positive for GluR1 and associated with synaptophysin are also positive for the β_2AR (second bar; a total of 329 synapses in 15 fields in stratum radiatum 25–100 μm away from the pyramidal cell layer from three adult s.d. rats (five fields per rat) were analysed). (**C**) Post-embedding immunogold staining for the β_2AR in PFC. (a) Three immunopositive axospinous synapses in a single field. (b) A large strongly immunolabelled synapse. Labelling is mainly over PSD, close to postsynaptic plasma membrane ($n=2$ brains). (**D**–**F**) GluR1, but not NMDARs, specifically co-immunoprecipitate with β_2AR from rat brain lysates. Rat brain was solubilized with 1% Triton X-100 and cleared by ultracentrifugation before immunoprecipitation (500 μg protein per lysate sample) with the H-20 antibody against β_2AR or a control antibody and immunoblotting with antibodies against proteins indicated on the left side. The H-20 antibody, but not control IgG, immunoprecipitated the β_2AR (**D**; $n=3$) and GluR1 (**E**; $n=6$), but not NR2B (**E**; $n=2$). The β_2AR did not co-precipitate with NMDARs (**F**; $n=3$; 25 μg total lysate protein were loaded where indicated).

targeting of AMPARs (Chen *et al*, 2000; Schnell *et al*, 2002). Direct interactions between the β_2AR with PSD-95 and stargazin with both PSD-95 and GluR1 could establish a physical link between the β_2AR and AMPARs (Figure 2C).

To test whether stargazin links the β_2AR to GluR1 through PSD-95 in neurons, we evaluated whether co-immunoprecipitation of GluR1 with the β_2AR depends on the presence of stargazin. Stargazer mice ($stg^{-/-}$) lack functional stargazin, the prevailing TARP in adult cerebellum (Chen *et al*, 2000; Tomita *et al*, 2003; Menuz and Nicoll, 2008; Menuz *et al*, 2008). GluR1 co-immunoprecipitated with the β_2AR from cerebral cortex and cerebellum from wild-type mice (Figure 2D, top left panel). In $stg^{-/-}$ mice, GluR1 co-immunoprecipitated with the β_2AR from cortex, but not from cerebellum (Figure 2D, top right panel). These results indicate a requirement for stargazin for association of the β_2AR with GluR1 in the cerebellum, but not cortex, consistent with published evidence that other TARPs substitute for stargazin in cortex.

As the β_2AR forms a complex with GluR1, but not with NMDAR, that depends on stg and PSD-95 and their homologues, the interaction of the β_2AR with PSD-95 or its homologues is governed by other interactions of PSD-95. In other words, it is controlled by the immediate molecular environment of PSD-95. That only certain combinations of binding partners for complex formation with PSD-95 are realized *in vivo* seems to be critical to avoid physiologically undesirable assemblies or, worse, chaos by random complex formation.

β_2AR–GluR1 complex also contains G_s and adenylyl cyclase

Association of the β_2AR with GluR1 could allow selective and spatially restricted signalling. If so, the trimeric G_s protein, adenylyl cyclase, and PKA must also be localized near GluR1. PKA is structurally and functionally linked to GluR1 through

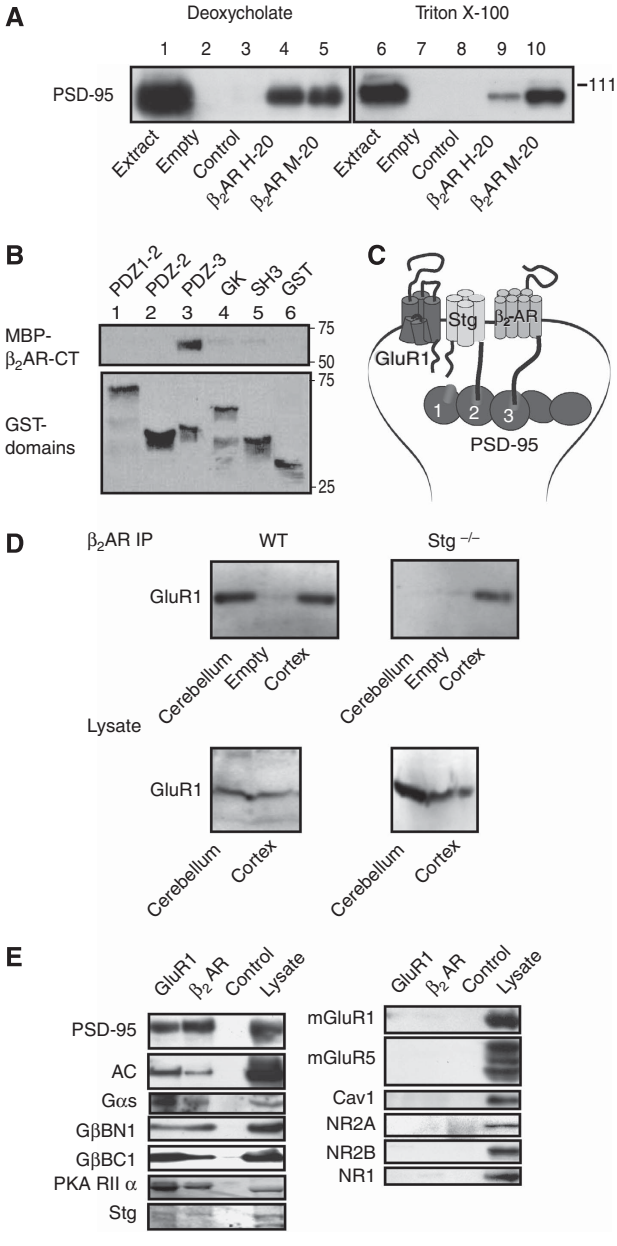

Figure 2 GluR1 forms a complex with the β_2AR through PSD-95 and stargazin, which also contains G_s and adenylyl cyclase. (**A**) Rat brains were extracted with 1% deoxycholate (left) and 1% Triton X-100 (right) before immunoprecipitation with two different antibodies against β_2AR (H-20, M-20) or control IgG, followed by immunoblotting with anti-PSD-95 ('JH62092' in Sans *et al* (2000); $n=4$). Specificity of the observed co-immunoprecipitation of PSD-95 with β_2AR (lanes 4,5,9,10) is indicated by a lack of PSD-95 signal in the control IgG samples (lanes 3 and 8). (**B**) GST fusion proteins of the PDZ1–2, PDZ2, PDZ3, SH3 and GK domains of PSD-95 and GST alone were immobilized on glutathione Sepharose and incubated with MBP fusion protein of the full cytosolic C-terminus of the human β_2AR (MBP-β_2AR-CT) before washing and immunoblotting with anti-MBP antibodies. MBP-β_2AR-CT bound strongly and specifically to the third PDZ domain (upper panel lane 3), but not to other domains of PSD-95 or to GST alone (lane 6). Reprobing with anti-GST antibodies shows that the different GST fusion proteins were present in comparable amounts (lower panel; $n=8$). (**C**) Schematic illustration of the β_2AR–GluR1 complex. Stg or one of its homologues in the AMPAR complex binds with the C-terminus to the first two PDZ domains of PSD-95 or one of its homologues. PSD-95 interacts with its third PDZ domain with the C-terminus of the β_2AR. (**D**) Loss of stargazin dissociates GluR1 from β_2AR. Triton X-100 extracts of cortices and cerebella of wild-type and litter-matched stargazer ($Stg^{-/-}$) mice were cleared by ultracentrifugation before immunoprecipitation of β_2AR and immunoblotting with anti-GluR1 antibodies. GluR1 co-immunoprecipitated with β_2AR from both cortex and cerebellum of wild-type mice (upper left panel) and with the β_2AR from cortex, but not cerebellum of $stg^{-/-}$ mice (upper right panel). Lower panels indicate that similar amounts of GluR1 were present in the various extracts. Similar results were obtained in three independent experiments with three wt and three $stg^{-/-}$ mice. (**E**) Association of G_s and adenylyl cyclase with the β_2AR–AMPAR complex. Triton X-100 extracts of crude rat forebrain membrane fractions were cleared by ultracentrifugation before immunoprecipitation with antibodies against GluR1 (lane 1), β_2AR (lane 2), or a non-specific control IgG (lane 3), followed by immunoblotting for the proteins indicated on the left side (Leonard *et al*, 1998; Davare *et al*, 2001). Anti-GluR1 and anti-β_2AR precipitated PSD-95 (positive control, $n=3$), adenylyl cyclase (AC, $n=3$), $G_{\alpha s}$ ($n=3$), and G_β. The latter was detected with two different antibodies that recognized the N- (BN1; $n=2$) and C-termini (BC1; $n=3$) of $G_{\beta 1-4}$ (left panels). PKA (here the RII_α subunit; $n=2$) and Stg ($n=4$) were also present in GluR1 and β_2AR precipitates. The metabotropic glutamate receptors mGluR1 ($n=3$) and mGluR5 ($n=3$), caveolin 1(Cav1; $n=3$) and the NMDA receptor subunits NR2A ($n=1$), NR2B ($n=3$), and NR1 ($n=1$) did not co-immunoprecipitate with either GluR1 or β_2AR (right panels), although all proteins were clearly detectable in lysate (lane 4). All immunoprecipitations were made from lysate samples containing 500 μg total protein; lysate aliquots containing 25 μg protein were loaded when indicated.

the A kinase anchor protein, AKAP150 (Colledge *et al*, 2000; Tavalin *et al*, 2002). AKAP150 associates with SAP97 (Colledge *et al*, 2000; Tavalin *et al*, 2002), which in turn binds directly to the C-terminus of GluR1 (Leonard *et al*, 1998). Figure 2E illustrates that G_s and adenylyl cyclase are also associated with GluR1: immunoprecipitation of either GluR1 or the β_2AR co-precipitated $G_{\alpha s}$, G_β, and adenylyl cyclase in extracts from total forebrain (left upper panels) as well as specifically from PFC and cerebellum (Supplementary Figure 1A). PKA and stargazin also co-precipitated with GluR1 and the β_2AR under these conditions (Figure 2E, left lower panels) as did GluR2 as tested in PFC and cerebellar extracts (Supplementary Figure 1A). As stargazin expression is low in forebrain (Tomita *et al*, 2003), immunoreactive signals are low in lysate and immunoprecipitates from forebrain. In contrast to these proteins, several other proteins that are likewise concentrated at the postsynaptic site did not co-immunoprecipitate with GluR1 or the β_2AR, including the metabotropic glutamate receptors mGluR1 and mGluR5, and the NMDAR subunits NR1, NR2A, and NR2B (Figure 2E, right panels). The plasma membrane raft marker caveolin 1 was also absent in these immunoprecipitates. Control IgG did not precipitate PSD-95, adenylyl cyclase, $G_{\alpha s}$, G_β, PKA, and stargazin. Therefore, we conclude that their co-immunoprecipitation with GluR1 and the β_2AR is specific.

Regulation of GluR1 S845 phosphorylation by associated β_2AR

By phosphorylating S845 on the intracellular COOH-terminal region of GluR1 (Roche *et al*, 1996), PKA promotes activity-driven synaptic targeting of GluR1 (Esteban *et al*, 2003). To determine whether β_2AR, G_s, adenylyl cyclase, PKA, and GluR1 are organized into a functional complex, primary hippocampal cultures were treated with the β-adrenergic agonist isoproterenol (ISO; 3 μM, 15 min). This treatment increased phosphorylation of S845 of GluR1 in hippocampal neurons (Figure 3A and B). The increase was attenuated with the highly selective β_2AR antagonist ICI118551 (1 μM), which by itself reduced basal S845 phosphorylation in some, but not all experiments. We next tested whether the β_2AR–GluR1 interaction is necessary for S845 phosphorylation, as pre-

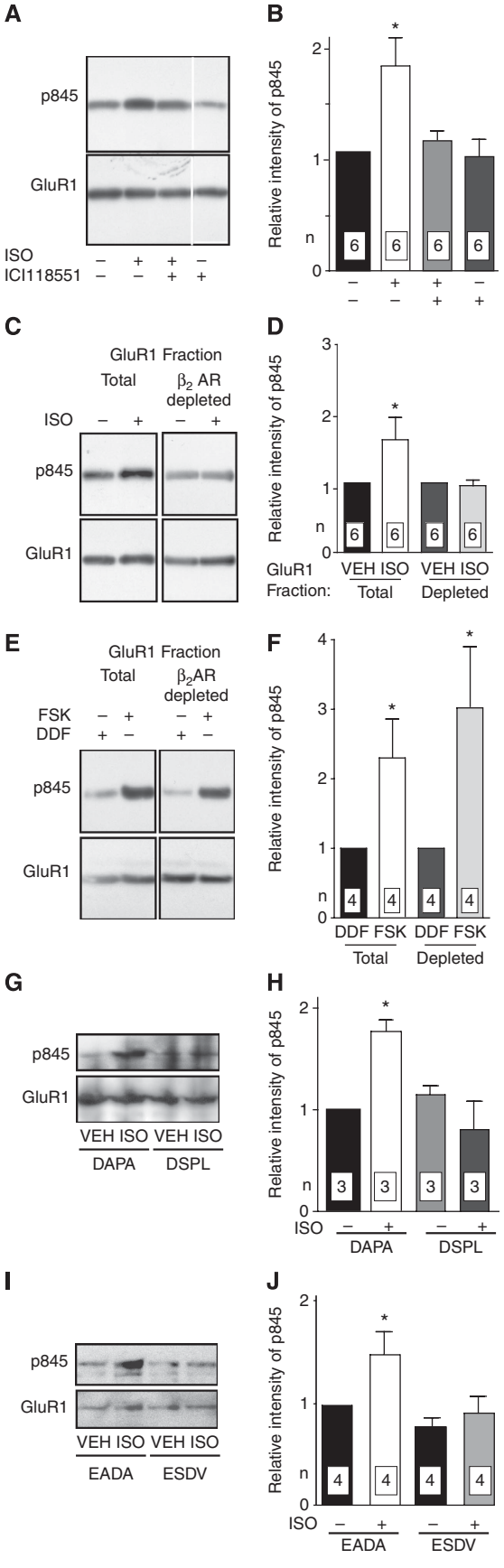

Figure 3 Localized regulation of GluR1 S845 phosphorylation by the β_2AR. Primary hippocampal cultures (18 DIV) were treated with vehicle (VEH), 3 μM ISO, 10 μM forskolin (FSK), or 10 μM 1,9-dideoxyforskolin (DDF; inactive forskolin homologue) for 15 min. Cultures were extracted with Triton X-100 and cleared by ultracentrifugation. GluR1 was immunoprecipitated directly or after pre-immunoprecipitation of β_2AR complexes (H-20) before immunoblotting with antibodies against phosphorylated S845 (top) and total GluR1 (bottom). Immunosignals were quantified by densitometry. Phospho-S845 (pS845) signals were corrected with respect to total GluR1 signals and normalized to control. (**A**, **B**) ISO significantly increased S845 phosphorylation. Pre-treatment for 15 min with 1 μM ICI118551-blocked ISO-induced phosphorylation. All lanes are from same blot and exposure, but non-relevant lanes have been removed between lane 3 and 4. (**C**–**F**) After treatments, culture extracts were split into two equal portions. In contrast to the total GluR1 population (left pairs in **C**, **D**), GluR1 remaining after depletion of GluR1–β_2AR complexes by pre-immunoprecipitation with H-20 showed no ISO-induced increase in S845 phosphorylation (right pairs in **C**, **D**), although forskolin stimulated S845 phosphorylation in both the total and the GluR1–β_2AR-depleted GluR1 populations (**E**, **F**). (**G**–**J**) Pre-treatment for 2 h with membrane-permeant DSPL and ESDV peptides, but not their inactive analogues DAPA and EADA (1 μM each) prevented induction of S845 phosphorylation by ISO. $^*P<0.05$ compared with control treatments; error bars: s.e.m.; *n*: number of independent experiments.

dicted if signalling from the β_2AR to the AMPAR through PKA is localized. After treatment with vehicle or ISO and extraction with Triton X-100, each sample was divided into two equal halves. One half was mock treated before immunoprecipitation of GluR1 to assess the total GluR1 population. The other half was first depleted of GluR1 that was associated with the β_2AR by immunoprecipitation with anti-β_2AR antibody. The resulting supernatant lacking β_2AR–GluR1 complexes was then used for immunoprecipitation with anti-GluR1. As before, ISO treatment induced S845 phosphorylation in the total GluR1 pool, but no such increase in phosphorylation was observed for the GluR1 pool from which β_2AR-associated GluR1 had been removed (Figure 3C and D). An analogous experiment with forskolin (10 μM, 15 min), a direct activator of adenylyl cyclase, led to increased S845 phosphorylation in the total GluR1 as well as the β_2AR-depleted GluR1 populations (Figure 3E and F). These results indicate that a substantial fraction of GluR1 is available for phosphorylation by PKA on S845 on massive stimulation of cAMP production even if not associated with the β_2AR. However, activation of the β_2AR leads to selective phosphorylation of β_2AR-linked GluR1.

To further test whether the complex formation between β_2AR and GluR1 is necessary for efficient signalling, cultures were pre-treated for 2 h with the membrane-permeable peptide 11R-QGRNSNTND**SPL** ('DSPL'). This peptide mimics the extreme C-terminus of the β_2AR, which interacts with the third PDZ domain of PSD-95, and disrupts the co-immunoprecipitation of the β_2AR with GluR1 (Supplementary Figure 1B). It had little effect on the co-immunoprecipitation of PSD-95 with GluR1, as expected, because the latter engages PDZ domains 1 and 2 of PSD-95 and its homologues. Binding selectivities of the first and second PDZ domains of PSD-95 and related proteins such as SAP97 and SAP102 are very similar to each other, but differ from those of the third PDZ domains (Lim *et al*, 2002, 2003). Control treatments were performed with its inactive analogue 11R-QGRNSNTND**APA** ('DAPA') altered at the 0 and −2 position (in bold), which are critical for PDZ domain binding. Subsequent incubation with ISO (3 μM, 15 min) led to increased S845 phosphorylation only in samples pre-treated with DAPA, but not in those pre-treated with DSPL (Figure 3G and H). A second pair of peptides gave analogous results: 11R-VYKKMPSI**ESDV** ('ESDV') and its inactive analogue 11R-VYKKMPSI**EADA** ('EADA') is based on the C-terminus of NR2A. ESDV has optimal binding affinity for PDZ1 and 2 of PSD-95 and its homologues (Lim *et al*, 2002) and effectively blocks PDZ1 and 2 interactions (Lim *et al*, 2003). The latter conclusion had been based on immunoprecipitation experiments of PSD-95 with the NMDAR and was now confirmed for the co-immunoprecipitation of PSD-95 with GluR1, which was disrupted as expected (Supplementary Figure 1B). Pre-treatment with ESDV, but not EADA, prevented the ISO-triggered increase in S845 phosphorylation (Figure 3I and J). Collectively, these peptide experiments indicate that PSD-95 and its homologues structurally and functionally connect through PDZ domains the β_2AR to the GluR1–stargazin complex for S845 phosphorylation.

Increased surface expression of GluR1 by the associated β_2AR

The amount of GluR1 is increased at postsynaptic sites on stimulation of S845 phosphorylation by PKA (Swayze *et al*, 2004; Sun *et al*, 2005; Man *et al*, 2007). We asked whether the classic β-adrenergic signalling pathway controls postsynaptic GluR1 accumulation in hippocampal neurons using ectopically expressed GluR1 with superecliptic pHluorin (SEP) at its extracellular N-terminus. The pH-sensitive SEP–GluR1 signal was nearly completely quenched if the extracellular pH was lowered from 7.4 to 6.0 (Supplementary Figure 2), implying that the SEP–GluR1 signal was only detectable if SEP–GluR1 was present at the surface, but not in acidic intracellular organelles. The SEP–GluR1 fluorescence was stable for several hours under our imaging paradigm (data not shown). In initial experiments, 1 μM ISO in combination with the phosphodiesterase inhibitor 3-isobutyl-1-methylxanthine (IBMX; 250 μM) to enhance cAMP levels on β-adrenergic stimulation strongly increased surface expression of SEP–GluR1 at dendritic spines within 15 min, elevating both the intensity for individual puncta and the number of detectable puncta per dendritic length (Supplementary Figure 3). IBMX alone was without effect indicating that signalling was driven by ISO. The ISO effect was completely blocked if the β_2AR antagonist ICI118551 (1 μM) was added immediately before monitoring SEP–GluR1 signals. Subsequent experiments illustrate that a 5 min treatment with 1 μM ISO is sufficient for the full increase in synaptic SEP–GluR1 accumulation (Figure 4).

Similarly, ISO alone (10 μM, 15 min) elevated the number and intensity of GluR1-positive puncta detected by surface labelling of endogenous GluR1 with an antibody against its N-terminus (Figure 5). Double labelling with the synaptic marker synaptophysin confirmed that ISO-induced increases in GluR1 staining occurred at synapses (Figure 5A, B, D, E). This elevation was fully blocked by the β_2AR antagonist ICI118551, but not by the β_1AR antagonist ICI89406 (Figure 5F; Supplementary Figure 4). Disrupting binding of stargazin and its homologues to PDZ1 and 2 of PSD-95 and its homologues with the ESDV peptide or of the β_2AR to PDZ3 of PSD-95 with the DSPL peptide also prevented ISO-induced increases in GluR1 surface expression (Figure 5G; Supplementary Figure 4). The corresponding control peptides EADA and DAPA had no effect (Figure 5G). ICI118551 and more so DSPL (but for unknown reasons not ESDV) showed a clear tendency towards reducing GluR1 surface labelling under control conditions by themselves, which reached statistical significance for changes in synaptic GluR1 puncta frequency (Figure 4D). These results suggest that basal activity of the β_2AR can enhance GluR1 surface expression under non-stimulated conditions (see also effect of ESDV and DSPL on EPSC in PFC below). At the same time, none of the peptides affected the localization of the β_2AR, PSD-95, or the NMDAR under control conditions (Supplementary Figure 5). These findings exclude a widespread basal effect of these peptides and reassure that the actions of DSPL and ESDV on β_2AR-mediated effects are due to specific interference with the β_2AR–GluR1 assembly. We conclude that stimulation of the β_2AR promotes surface expression of GluR1 that resides in a complex with the β_2AR held together by PSD-95.

Stimulation of the β_2AR up-regulates postsynaptic AMPAR responses

Activation of βARs can modestly increase synaptic transmission at glutamatergic synapses in hippocampal slices within minutes, although this increase varied and was not observed in all recordings (Dahl and Sarvey, 1989; Thomas *et al*, 1996;

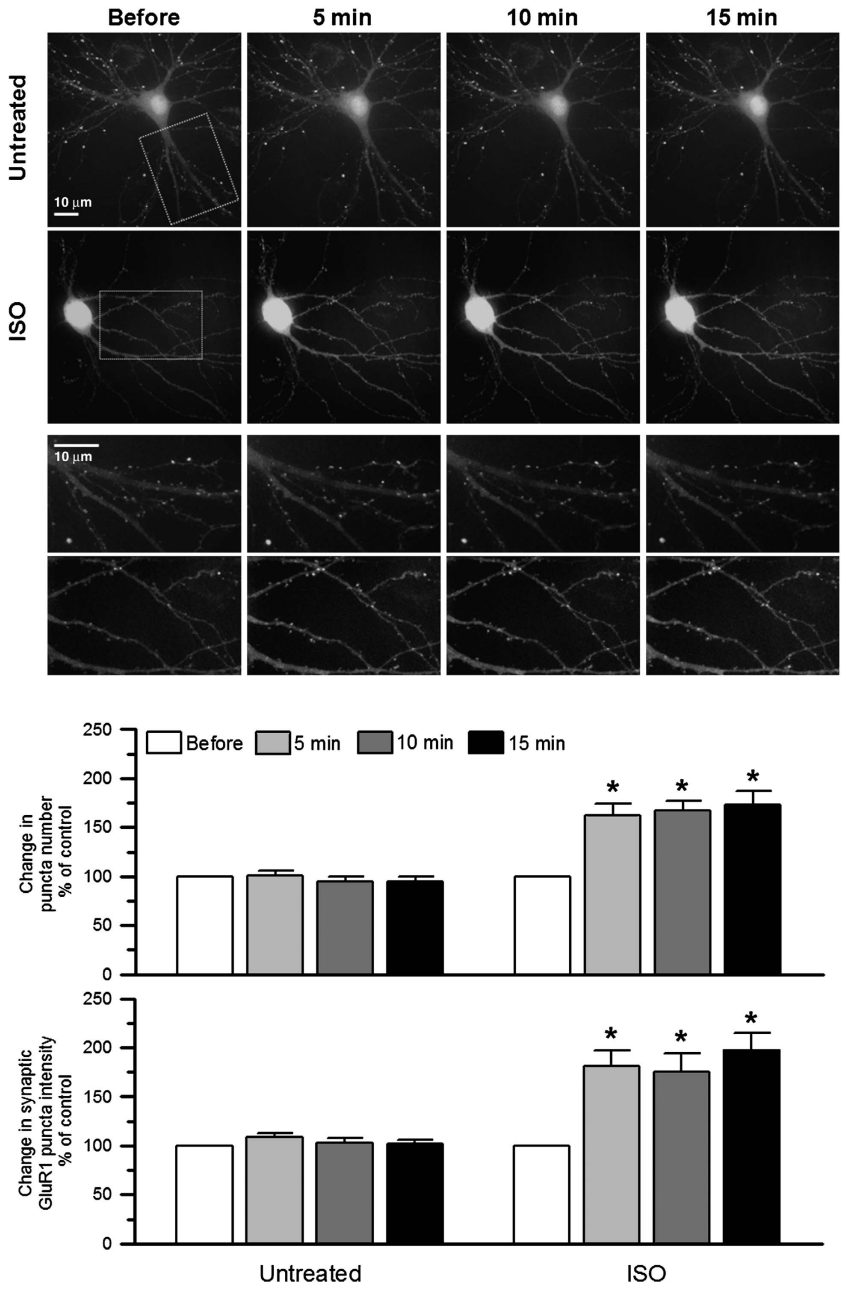

Figure 4 ISO increases SEP–GluR1 surface expression in dendritic spines. Primary hippocampal cultures were transfected with SEP–GluR1 at 5–7 DIV and imaged at 21DIV. ISO (1 μM) increased density and signal intensity of SEP–GluR1 puncta within 5 min, which otherwise remained constant under untreated control conditions. $^*P<0.05$ compared with control; error bars: SEM. In each case, a minimum of 5 dendrites from 15 neurons in 3 different experiments were analysed.

Katsuki *et al*, 1997; Winder *et al*, 1999; Gelinas and Nguyen, 2005). Similarly, we found that 10 μM ISO increased fEPSP initial slope in acute hippocampal slices in 14 out of 23 slices (Supplementary Figure 6A). Averaging all responses gave a statistically significant increase by 24% (Supplementary Figure 6B). Paired-pulse facilitation was unaltered, suggesting that ISO acted postsynaptically (Supplementary Figure 6C).

As ISO-induced up-regulation of fEPSPs was variable in hippocampal slices, we evaluated its effect in the PFC, which receives stronger noradrenergic innervation than the hippocampus (Minzenberg *et al*, 2008). In acute PFC slices, 10 μM ISO caused a robust and lasting increase of EPSC amplitudes by >50% (Figure 6A), which was completely blocked by the β_2AR antagonist ICI118551 (Figure 6B). ICI118551 itself reduced EPSC amplitude by 14.4 ± 2.6% (not illustrated), presumably reflecting basal β_2AR activity. Paired-pulse facilitation was unaltered in PFC slices (Figure 6C), indicating that the ISO effects were postsynaptic. ISO also significantly increased mEPSC amplitude (Figure 6D and E), but had no effect on mEPSC frequency (Figure 6E), decay time constant (control: 4.7 ± 0.5 ms; $n=6$; ISO: 4.8 ± 0.32 ms; $n=5$; wash: 4.7 ± 0.36 ms; $n=5$), or the 10–90% rise time (control: 2.7 ± 0.05 ms; $n=6$; ISO: 2.7 ± 0.05 ms; $n=5$; wash: 2.8 ± 0.07 ms; $n=5$). As the ISO effect was more robust and predictable in

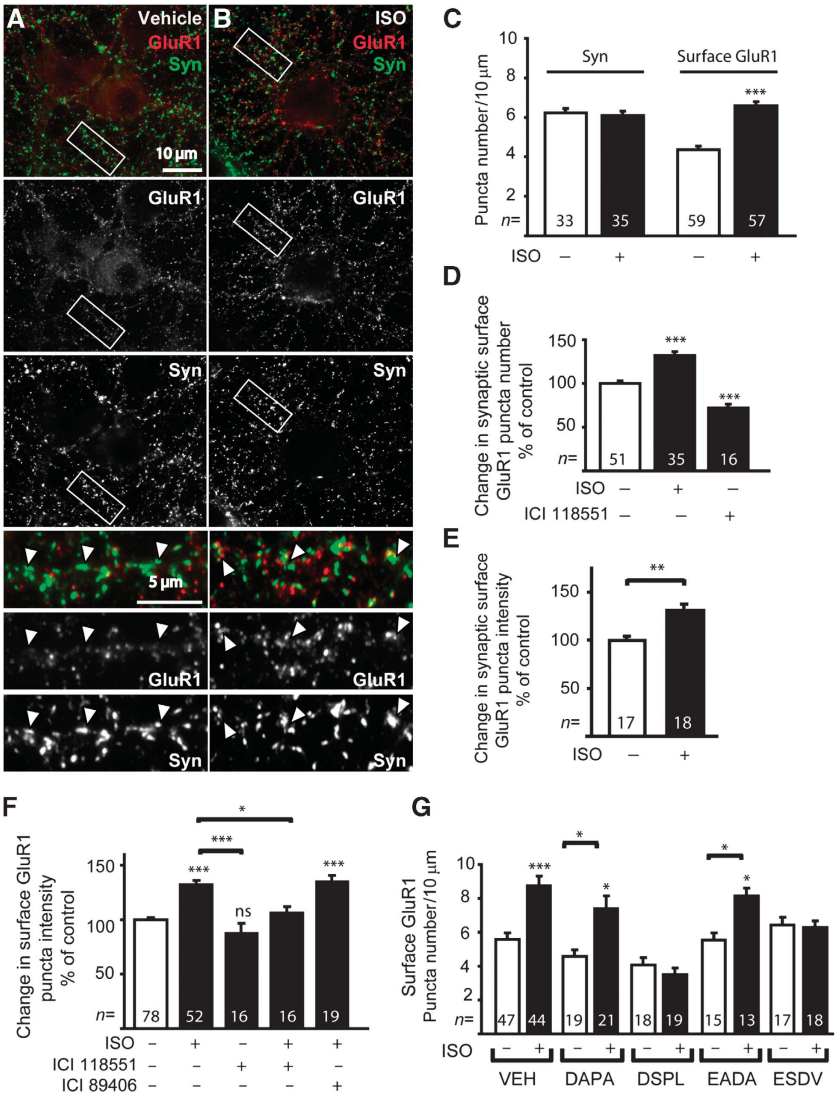

Figure 5 GluR1-associated β_2AR stimulates surface expression of endogenous GluR1. (**A**, **B**) Primary hippocampal cultures (18 DIV) were treated with vehicle (VEH) or 10 µM ISO for 15 min, surface labelled with the N-terminal GluR1 antibody (red), fixed, permeabilized, and counter labelled with anti-synaptophysin antibody (green). ISO caused a significant increase in surface expression of GluR1 compared with control cells treated with vehicle as indicated by quantification of total density of GluR1 puncta (**C**), density of synaptic GluR1 puncta (**D**; puncta that are colocalized with synaptophysin puncta), and GluR1 staining intensity at synaptic puncta (**E**). The ISO effect was blocked by 15 min pre-treatment with the β_2AR-selective antagonist ICI118551 (1 µM), but not the β_1AR-selective antagonist ICI89406 (1 µM; **F**). (**G**) Pre-treatment for 1 h with membrane-permeant D**S**P**L** and E**S**D**V** peptides, but not their inactive analogues D**A**P**A** and E**A**D**A** prevented ISO from increasing GluR1 surface expression. $^*P<0.05$; $^{**}P<0.001$; $^{***}P<0.0001$ compared with controls treatments or as indicated; error bars: s.e.m.; *n*: number of neurons analysed in at least three independent experiments for each condition.

PFC than hippocampus slices, we used the PFC for further mechanistic studies.

Up-regulation of AMPAR responses in PFC by the β_2AR depends on PKA

To ensure that the ISO response is mediated by PKA, the highly specific PKA inhibitory PKI peptide PKI_{5-22} was included in the patch pipette for both evoked EPSC and mEPSC analysis. Dialysis of PKI_{5-22} (40 µM) gradually reduced AMPAR-EPSC by 30.7 ± 4.4% ($n=9$) and blocked the increasing effect of ISO (10.1 ± 3.9%; $n=9$; Figure 6F; Supplementary Figure 7A). A scrambled control peptide had no effect on EPSC (5.8 ± 1.5%; $n=5$), and the ISO effect remained intact (51.6 ± 3.5%; $n=5$).

Dialysis of PKI_{5-22}, but not scrambled peptide, also reduced mEPSC amplitude (control: 14.4 ± 0.8pA; $n=8$; PKI_{5-22}: 10.2 ± 0.8pA; $n=8$; scrambled peptide: 13.8 ± 0.6pA; $n=6$; Figure 6G; Supplementary Figure 7C and E), but not frequency (control: 3.9 ± 0.4 Hz; $n=8$; PKI_{5-22}: 3.8 ± 0.4 Hz; $n=8$; scrambled peptide: 3.3 ± 0.4 Hz; $n=6$; Supplementary Figure 7D and F). PKI_{5-22} abolished the increasing effect of ISO on mEPSC amplitude (PKI_{5-22}: 10.2 ± 0.8pA; $n=8$; PKI_{5-22} + ISO: 11.6 ± 0.9pA; $n=8$; Supplementary Figure 7E), whereas the effect was intact in scrambled peptide-injected neurons (scrambled peptide: 13.8 ± 0.6pA; $n=6$; scrambled peptide + ISO: 19.3 ± 0.9pA; $n=7$, $P<0.001$, ANOVA). ISO had also no effect on mEPSC frequency in the presence of PKI_{5-22} (PKI_{5-22}: 3.8 ± 0.4 Hz;

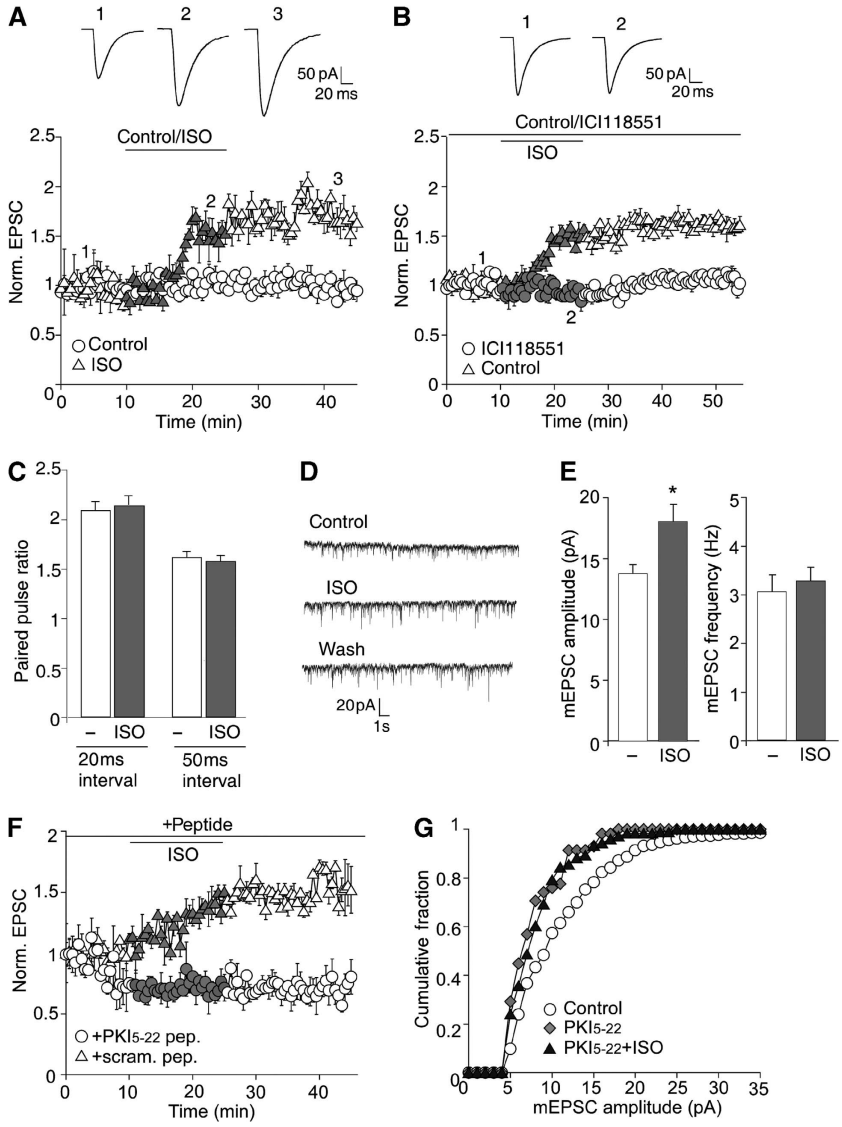

Figure 6 β_2AR stimulation increases postsynaptic AMPAR-mediated EPSCs in PFC slices. (**A**) During bath application of ISO (10 μM; grey symbols), the amplitude of evoked AMPAR-EPSC in PFC pyramidal neurons gradually increased by 53 ± 7.7% ($n = 7$), lasting for at least 20 min (after 20 min washout: 71.4 ± 23.7%; $n = 7$). (**B**) Bath application of the β_2AR antagonist ICI118551 (1 μM) prevented the ISO-triggered increase in AMPAR-EPSC amplitude (109.5 ± 1.8% of control, $n = 12$), compared with control cells without the antagonist (149.4 ± 4.3%, $n = 11$). (**C**) Paired-pulse facilitation (PPF) is unchanged in neurons treated for 15 min with 10 μM ISO (20 ms interval: control: 2.08 ± 0.1, ISO: 2.14 ± 0.1; $n = 5$; 50 ms interval: control: 1.6 ± 0.06, ISO: 1.6 ± 0.06; $n = 7$; paired-pulse ratio was determined by dividing the amplitude of the second EPSC to the first EPSC). (**D**, **E**) Miniature EPSC (mEPSC) recordings from PFC slices. Bath perfusion of ISO (10 μM, 15 min) increased mEPSC amplitude by 28.6 ± 2.7% (from 13.8 ± 0.7 pA to 18.0 ± 1.4 pA; $n = 6$), which remained elevated for at least 20 min (after 20 min washout: 27 ± 2.3%; $n = 6$). However, there was no significant change for mEPSC frequency (before ISO: 3.1 ± 0.35 Hz; with ISO: 3.3 ± 0.3 Hz; $n = 9$). (**F**, **G**) PKA is required for up-regulation of AMPAR responses by ISO. Injection of PKI_{5-22}, but not scrambled peptide (40 μM) inhibited EPSC (**F**) and mEPSC amplitudes (**G**) and prevented ISO from increasing the amplitudes.

$n = 8$; PKI_{5-22} + ISO: 3.9 ± 0.41 Hz; $n = 8$) or scrambled peptide (scrambled peptide: 3.3 ± 0.4 Hz; $n = 6$; scrambled peptide + ISO: 3.4 ± 0.16 Hz; $n = 7$).

ISO induces a lasting increase in S845 phosphorylation through adenylyl cyclase

As the increase in EPSC and mEPSC amplitude by ISO in PFC remained beyond washout of ISO, we tested whether the same would be true for S845 phosphorylation. Incubation of acute PFC slices with 10 μM ISO lead to near maximal phosphorylation within 2 min (Supplementary Figure 8). Importantly, when slices were treated for 15 min with ISO followed by 15 min washout of ISO S845, phosphorylation remained elevated, which explains the continued heightened EPSC and mEPSC responses after removal of ISO.

To corroborate that ISO acts through adenylyl cyclase, which is part of the main signalling pathway downstream of the β_2AR and is present in the GluR1–β_2AR complex (Figure 2E; Supplementary Figure 1A), PFC slices were treated with 10 μM ISO for 15 min in the absence and presence of 20 μM SQ22536, an adenylyl cyclase inhibitor. The increase in S845 phosphorylation by ISO was reduced by >50%, indicating that it was largely mediated by adenylyl cyclase (not illustrated).

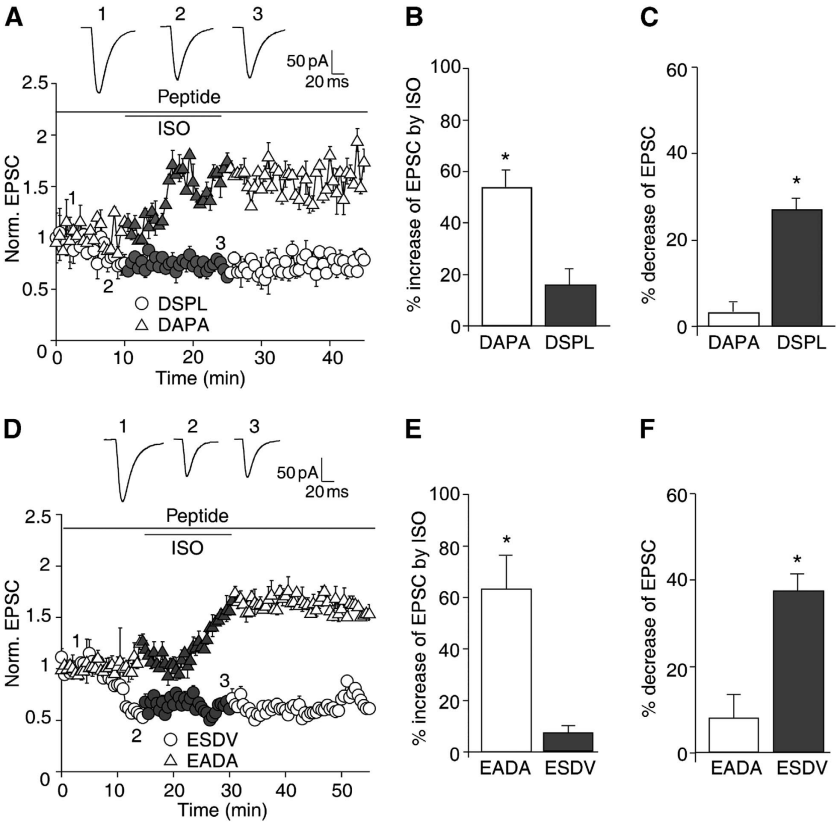

Figure 7 Peptides that disrupt the β_2AR–AMPAR interaction specifically prevent the ISO-induced increase in EPSCs amplitude in PFC slices. (**A**–**C**) Basal AMPAR-EPSC amplitudes were significantly reduced by injection of the D**S**P**L** peptide (50 μM) by 25.2 ± 4.9% ($n = 5$), but not by the control D**A**P**A** peptide (50 μM; 3.2 ± 2.2% reduction; $n = 5$). D**S**P**L** diminished the ISO response to an increase of 15.7 ± 5.9% ($n = 7$), but D**A**P**A** did not cause any significant reduction (increase was 54.3 ± 6.6%; $n = 6$). (**D**–**F**) Basal AMPAR-EPSC amplitudes were significantly reduced by injection of the E**S**D**V** peptide (50 μM) by 37.5 ± 4% ($n = 10$), but not by the control E**A**D**A** peptide (50 μM; 8.8 ± 4.7% reduction; $n = 10$). E**S**D**V** diminished the ISO response to an increase of 6.8 ± 2.7% ($n = 10$), but D**A**P**A** did not cause any significant reduction (increase was 62.7 ± 12.9%; $n = 10$).

Up-regulation of AMPAR responses by ISO requires β_2AR–AMPAR association

The DSPL and ESDV peptides were used to test whether up-regulation of AMPAR-mediated EPSCs by the β_2AR depends on PSD-95 binding to TARPs and the β_2AR. Infusion of either peptide through the whole-cell recording electrode prevented ISO from increasing EPSCs (Figure 7). Similar to ICI118551, both peptides decreased EPSC amplitude by themselves, further supporting the notion that basal activity of GluR1-associated β_2AR enhances AMPAR responses under resting conditions in PFC slices. The corresponding control peptides (DAPA and EADA) showed none of these effects.

Up-regulation of AMPAR responses by the β_2AR depends on intact exocytosis

Phosphorylation of S845 up-regulates GluR1 surface expression by promoting its insertion into the plasma membrane (Ehlers, 2000; Swayze *et al*, 2004; Sun *et al*, 2005; Oh *et al*, 2006; Man *et al*, 2007). It also might increase AMPAR channel activity (Roche *et al*, 1996). To evaluate whether the β_2AR up-regulates AMPAR responses mainly by augmenting surface expression, we used two different reagents that inhibit exocytosis. *N*-ethylmaleimide (NEM) inhibits NEM-sensitive factor, and thereby membrane fusion events required for trafficking of surface proteins to the plasma membrane. Earlier work established that post-synaptic injection of NEM blocks LTP without affecting basal postsynaptic responses (Lledo *et al*, 1998). Similarly, NEM infusion did not alter EPSCs in PFC neurons under basal conditions, but prevented up-regulation of EPSCs by ISO (Figure 8A and C). Botulinum neurotoxin B (BoTox) and tetanus toxin (TeTox) block exocytosis by proteolytic cleavage of synaptobrevin/VAMP2, which is critical for exocytosis (Schiavo *et al*, 2000). Injection of the catalytically active BoTox or TeTox light chain does not reduce basal postsynaptic responses, but abrogates LTP (Lledo *et al*, 1998; Lu *et al*, 2001). Similar to NEM, BoTox blocked the ISO-triggered increase in EPSC amplitude (Figure 8B and C). These data show that ISO increases postsynaptic AMPAR responses mainly by promoting insertion of AMPARs into the cell surface.

Discussion

Our data indicate that the β_2AR, G_s, and adenylyl cyclase form a supramolecular signalling complex with GluR1, which is known to associate with PKA and the antagonistic phosphatase PP2B through AKAP150, SAP97, and, alternatively, PSD-95 (Leonard *et al*, 1998; Colledge *et al*, 2000; Tavalin *et al*, 2002). Remarkably, only GluR1-containing complexes that are associated with β_2ARs are effectively regulated by β-adrenergic stimulation, showing that this assembly

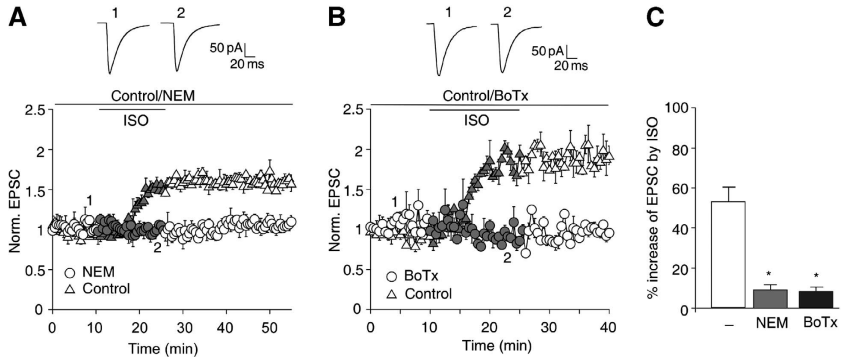

Figure 8 Exocytosis blockage prevents the ISO-induced increase in EPSCs amplitude in PFC slices. (**A**) Dialysis of NEM (5 mM) itself did not significantly alter AMPAR-EPSC amplitude (104.3 ± 1.4% of control; $n = 11$), but decreased the effect of ISO to an increase of 11.8 ± 2.6% stimulation ($n = 11$). (**B**) Dialysis of Botulinum neurotoxin (0.5 μM) itself did not significantly alter AMPAR-EPSC amplitude (102.8 ± 1.5%; $n = 8$), but reduced the effect of ISO to an increase of 10 ± 1.9% stimulation ($n = 10$). (**C**) Averages in changes of EPSC amplitudes from all experiments from panels A and B.

allows for highly localized control of GluR1 phosphorylation by the β_2AR.

Another study suggests that the β_1AR, but not β_2AR, regulates S845 phosphorylation (Vanhoose and Winder, 2003), contrasting our findings. The differences between this and our study that lead to this discrepancy outcome could be related to differences in the exact experimental system, though quite similar, or the high concentrations of the β_1 selective blocker betaxolol (10 μM) used in the other study at which isotype specificity could have been lost (e.g. Smith and Teitler, 1999; Sharif and Xu, 2004). In addition, there was no evidence presented that the ICI118551 batch was active in the other study. However, we do not want to exclude that the β_1AR can contribute to S845 phosphorylation under certain conditions.

Phosphorylation of S845 by PKA promotes GluR1 surface expression because of a combination of reduced internalization rate and increased re-insertion rate (Ehlers, 2000; Man *et al*, 2007). We now show that, upstream of PKA, activation of the β_2AR specifically augments the synaptic expression of GluR1. S845 phosphorylation might also enhance the activity of GluR1-containing AMPARs by increasing their open probability (Banke *et al*, 2000), which could have contributed to the increase in AMPAR responses we observed in acute hippocampal and PFC slices. However, ISO-induced increases in the PFC were largely blocked by infusion of BoTox indicating that increased activity of AMPARs that were already present at postsynaptic sites could have made only a modest contribution.

The increase in GluR1 surface expression contrasts with the decrease of β_2AR typically induced by β_2AR ligands. However, agonist-induced internalization typically reduces surface β_2AR by $<50\%$, and in some cases as little as 10% (e.g. Shenoy *et al*, 2006). Furthermore, association of the β_1AR with PSD-95 inhibits its ligand-induced internalization (Xu *et al*, 2001). Analogously, the β_2AR might be resistant to internalization when forming a complex with PSD-95, stargazin, and GluR1.

The β_2AR-dependent increase in S845 phosphorylation emerges as an important consequence of adrenergic activation throughout the brain. β-adrenergic stimulation can increase synaptic transmission at glutamatergic synapses in hippocampal slices within minutes, although that is not observed in all experiments (Dahl and Sarvey, 1989; Thomas *et al*, 1996; Katsuki *et al*, 1997; Winder *et al*, 1999; Gelinas and Nguyen, 2005). At the same time, β-adrenergic activation fosters induction of LTP, which can transform a reversible increase in synaptic strength into a lasting one (Thomas *et al*, 1996; Katsuki *et al*, 1997; Winder *et al*, 1999; Lin *et al*, 2003; Gelinas and Nguyen, 2005). Recent work indicates that norepinephrine and emotional stress induce phosphorylation of GluR1 S845 and to a lesser degree on S831, a phosphorylation site for PKC and CaMKII (Hu *et al*, 2007). Mutating both sites to alanine interferes with norepinephrine-dependent LTP induction by a 10 Hz/90 s tetanus and fear conditioning by a modest conditioning paradigm (Hu *et al*, 2007). Furthermore, a single mutation of S845 to alanine prevents ISO from priming neurons in the visual cortex for spike time-dependent potentiation (Seol *et al*, 2007).

In closing, the localized signalling from the β_2AR to GluR1 described here represents a critical regulatory mechanism for postsynaptic functions linking the noradrenergic and glutamatergic systems in the brain. This mechanism is likely to have a major function in mediating noradrenergic effects on the brain, including heightened arousal and facilitation of synaptic plasticity and learning (Cahill *et al*, 1994; Nielson and Jensen, 1994; Berman and Dudai, 2001; Strange *et al*, 2003; Strange and Dolan, 2004; Hu *et al*, 2007). These findings also illustrate the importance of noradrenergic innervation of the hippocampus, although this innervation is typically eliminated in experiments using hippocampal slices, but must not be neglected. Finally, the characterization of the β_2AR–G_s–adenylyl cyclase–PKA–GluR1 complex reported here illuminates the capability of the β_2AR to drive spatially restricted generation of cAMP. This work firmly establishes the concept of locally restricted and thereby highly selective signalling by cAMP, through formation of supramolecular signalling complexes.

Materials and methods

Reagents and antibodies

ISO, ICI118551, forskolin, dideoxyforskolin, and NEM were from Sigma and ICI89406 from Biotrend Chemicals Inc. A peptide derived from the C-terminus of GluR1 (MSHSSGMPLGATGL) was purified by HPLC, cross-linked with glutaraldehyde to bovine serum albumin and injected into rabbits as described (Davare *et al*, 1999) to obtain anti-GluR1 antiserum. For immunoprecipitation of

GluR1, 2 μl of this serum were used in 0.5 ml extracts. For immunoblotting, this serum was diluted 1:1000. Antibodies against the extracellular N-terminus of GluR1 were from Oncogen Research, Bassoon from Stressgen, β_2AR (H-20 and M-20) from Santa Cruz, and $G_{\alpha s}$ from Upstate. Non-specific rabbit IgG was from Zymed. Anti-PSD-95 was produced earlier by us and corresponds to 'JH62092' in Leonard and Hell (1997), Leonard *et al* (1999), Sans *et al* (2000), and Davare *et al* (2001). All other antibodies including those against G_β, pan-adenylyl cyclase, mGluR1, mGluR5, caveolin-1, NR1, NR2A, and NR2B and the phospho-specific antibody against S845 were as described earlier (Leonard and Hell, 1997; Leonard *et al*, 1999; Sans *et al*, 2000; Davare *et al*, 2001; Lu *et al*, 2007). The membrane-permeable peptides 11R-QGRNSNTND**S**P**L** (DSPL), 11R-QGRNSNTND**A**P**A** (DAPA), 11R-VYKKMPSIE**S**D**V** (ESDV), and 11R-VYKKMPSIE**A**D**A** (EADA) were custom synthesized by the W. M. Keck Biotechnology Resource Center, Yale University and HPLC purified. Botulinum Neurotoxin Type B Light Chain (BoTox) was from Listlabs. All other reagents were from the usual suppliers and of standard quality.

Immunocytochemistry

Adult male Sprague–Dawley rats were deeply anesthetized with sodium pentobarbital and perfused with 4% paraformaldehyde following NIH guidelines as described (Burette *et al*, 1999) and approved by the University of North Carolina. Fifteen minutes after the onset of fixation, material was flushed with normal saline. Brains were removed, tissue sections cut on a Vibratome and processed for multiple label immunofluorescence. After blocking, rabbit anti-β_2AR (1:10000; H-20) was added, followed by horseradish peroxidase-conjugated secondary antibody. Fluorophore-conjugated tyramide was then used to amplify the signal followed by PBS washes (Burette *et al*, 1999). Subsequently, standard double labelling with rabbit anti-GluR1 antibody (1:1000) and mouse-anti-synaptophysin (1:5000) was performed. Quantitative data were collected by confocal microscopy from stratum radiatum of hippocampal CA1, at least 25 μm from the pyramidal layer (Melone *et al*, 2005); 329 synapses from five fields from each of three rats were analysed for quantification of the number of β_2AR- and GluR1-labelled puncta (Melone *et al*, 2005). We considered only neuropil, avoiding somata and dendritic shafts. To focus specifically on synaptic labelling, we only considered immunopositive puncta clearly associated with puncta stained for synaptophysin.

Immunogold labelling

Pentobarbital-anesthetized adult rats were perfused with a mixture of 2% depolymerized paraformaldehyde and 2% glutaraldehyde in phosphate buffer, after a brief saline rinse, as per institutionally approved protocols and NIH guidelines. A total of 200 μm Vibratome sections were cryoprotected in 30% glycerol. Chunks of prefrontal/orbital cortex were plunge frozen in isopentane and dehydrated over several days at −60° in ethanol with 1% uranyl acetate, infiltrated with Lowicryl HM-20, and UV-polymerized at low temperature. Thin (~80–100 nm) sections were collected on nickel mesh grids and processed for immunogold labelling, using the M20 antibody at 1:1000 dilution, according to Phend *et al* (1992, 1995). Grids were examined on a Philips Tecnai transmission electron microscope.

Immunoprecipitation and immunoblotting

Sprague–Dawley rats were obtained from Harlan and homozygous stargazer mice and litter-matched wild-type control mice from Jackson Laboratories. The Animal Care and Use Committee of the University of Iowa approved all procedures involving animals. Forebrains, neocortices, or cerebella were homogenized in a 10-fold volume of Buffer A (150 mM NaCl, 10 mM EDTA, 10 mM EGTA, 10 mM Tris–HCl, pH 7.4, and protease inhibitors) containing 1% deoxycholate or 1% Triton X-100, and cleared from non-solubilized material by ultracentrifugation (minimally 250 000 *g* for 30 min) before immunoprecipitation with the C-terminal GluR1 antibody, H20 against the β_2AR, or an equivalent amount of non-specific rabbit IgG and subsequent immunoblotting with the indicated antibodies as described (Leonard and Hell, 1997; Leonard *et al*, 1999).

GST and MBP fusion proteins and pull-down assay

GST fusion proteins of the PDZ1–2 (residues 1–185), PDZ2 (156–248), PDZ3 (302–402), SH3 (431–500), and GK (534–724) domains of PSD-95 and an MBP fusion protein of the full cytosolic C-terminus of the human β_2AR (MBP-β_2AR-CT; residues 326–413) were expressed in *Escherichia coli* as described (Seabold *et al*, 2003). GST fusion proteins were bound to glutathione Sepharose 4B (Amersham), washed, incubated with MBP-β_2AR-CT for 90–120 min at 4°C in TBS (10 mM Tris, 150 mM NaCl, 0.1% TX100; pH 7.4), and washed. Immunoblotting was performed with a monoclonal anti-MBP antibody (NEB), stripped with SDS and dithiothreitol and reprobed with anti-GST antibody (Leonard *et al*, 1998).

Hippocampal cultures and phosphorylation studies

Hippocampal cultures were prepared from E18 embryonic Sprague–Dawley rats (Harlan) and maintained as described (Lim *et al*, 2003) using the B27-derived culture medium supplement NS21 (Chen *et al*, 2008). Cultures (DIV18) were pre-incubated for 15 min with the βAR antagonists ICI118551 (β_2AR; 1 μM) or ICI 89406 (β_1AR; 1 μM) if indicated before incubation with vehicle (water) versus ISO (1–3 μM) or forskolin (10 μM; from DMSO stock) versus 1,9-dideoxyforskolin (10 μM) for 15 min. For immunoprecipitation and analysis of S845, phosphorylation cultures were extracted with Triton X-100 in Buffer A containing the phosphatase inhibitors microcystin (0.4 μM) and para-nitriphenyl phosphate (100 μM). GluR1 was either directly immunoprecipitated or immunoprecipitated after initial immunoprecipitation with H-20 to remove GluR1–β_2AR complexes before subsequent immunoblotting with antibodies against GluR1 phosphorylated at S845 and, after stripping, with the C-terminal GluR1 antiserum. Relative phosphorylation levels were determined by densitometry of ECL signals on film. After scanning, pixel intensity of bands was quantified using Adobe Photoshop. Signals were in the linear range as shown earlier (Davare and Hell, 2003; Hall *et al*, 2006). Values were corrected for any variation in total GluR1 loaded and normalized to control treatment.

GluR1 surface labelling in hippocampal cultures

For surface labelling of GluR1, cultures were incubated after drug treatments with the N-terminal GluR1 antibody for 20 min at 37°C, fixed with 4% paraformaldehyde and 4 % sucrose for 15 min at room temperature, and incubated with Alexa 568 anti-rabbit secondary antibody (Molecular Probes) for 1 h at room temperature under non-permeabilized conditions (Swayze *et al*, 2004; Lise *et al*, 2006). For double labelling of GluR1 surface stained cultures, neurons were permeabilized with cold methanol for 5 min and incubated with anti-synaptophysin antibody overnight, followed by incubation with the appropriate secondary antibody. Images were taken using a ×63 objective on a Zeiss Axiovert M200 microscope. To allow comparison between different specimens, pictures were taken under the same settings. To correct for out-of-focus clusters within the field of view, focal plane (z) stacks were acquired and maximum intensity projections performed offline. Images were scaled to 16 bits and analysed in Northern Eclipse (Empix Imaging, Mississauga, Canada), by using user-written software routines (Gerrow *et al*, 2006; Lise *et al*, 2006). To measure puncta intensity and number per dendrite length, an experimenter blind to the treatment conditions manually outlined dendrites (at least 300 μM). Puncta were defined as sites of intensity at least twice the background. Average integrated puncta intensity was obtained by subtracting the average background grey from the average puncta grey intensities, which was then multiplied by the average puncta area. GluR1 puncta colocalizing with synaptophysin puncta were considered synaptic. At least eight neurons from two to three independent experiments were analysed. The s.e.m. values were calculated based on number of neurons examined. Two-tailed parametric Student's *t*-tests were performed to calculate the statistical significance of differences between two groups; one-way ANOVA was used to compare three or more groups, followed by Tukey-b *post hoc* analysis for multiple comparisons.

Monitoring SEP–GluR1 surface expression in hippocampal cultures

SEP was kindly provided by Dr Gero Miesenbock (Yale University, New Haven, CT). Its coding sequence was amplified by PCR (QuikChange protocol; Stratagene, La Jolla, CA) and inserted into the N-terminus of rat GluR1 after a signal peptide in pRK5 vector. Rat hippocampal cultures (DIV 5–7) were co-transfected with plasmids encoding DsRed (used to find transfeceted cells not to

bleach GFP) and SEP–GluR1 by the calcium phosphate method. At DIV 21, live cell images were captured with a system consisting of a BD CARVII™ confocal imager connected to a Leica DMIRE2 fluorescence microscope and a Hamamatsu EM CCD camera with filter sets. The X-Y coordinates of individual neurons on a mechanical X-Y stage were recorded within the IPLab4 software program, so that the same neuron could be located and photographed at different time periods during treatment. To maintain the neuron viability, imaging was carried out with a temperature-controlled stage (37°C) fitted with a CO_2 chamber set at 5% (Leica Microsystems). After capturing an image, the culture dish was immediately put back to a humidified 5% CO_2 incubator at 37°C for prolonged treatment.

Stacks of confocal images (not >25 z-planes) at 0.5 μm intervals were merged into one single image before analyses. All digital images were analysed with IPLab4 software (BD Biosciences). SEP–GluR1 puncta were defined as either dendritic protrusions with expanded heads that were 50% wider than their necks or regions of intensity at least twice the dendritic intensity. To quantify the SEP–GluR1 and dendritic intensity, the outline of puncta and the middle line on dendrites were manually drawn and these parameters were measured using the IPlab4 software. Average blank field intensity used as background was subtracted from these measurements to yield the actual intensity of SEP–GluR1. Data are expressed as mean ± s.e.m. of the indicated number of experiments. Statistical significance was determined using a paired *t*-test (Sigma plot 7.0; Systat software, San Jose, CA) in comparing the puncta density and fluorescence intensity before and after treatment of the same neuron.

Electrophysiological recording from PFC slices

All experiments were carried out with the approval of State University of New York at Buffalo Animal Care Committee following NIH guidelines. Slices were prepared from 3–5-week-old Sprague–Dawley rats as described before (for details see, Wu *et al*, 2005). In brief, animals were anesthetized by inhaling 2-bromo-2-chloro-1,1,1-trifluoroethane (1 ml/100g; Sigma) and decapitated. Brains were quickly removed and sliced (300 μm) with a Leica VP1000S Vibratome, whereas bathed in HEPES-buffered salt solution. Slices were then incubated for 1–5 h at room temperature (22–24°C) in a $NaHCO_3$-buffered saline (EBSS) bubbled with 95% O_2, 5% CO_2.

AMPAR-mediated synaptic transmission was monitored by standard whole-cell patch recordings from pyramidal neurons located in layer V in PFC slices (Yuen *et al*, 2007). PFC slices were perfused with oxygenated artificial cerebro-spinal fluid (ACSF) containing (mM) NaCl (130), $NaHCO_3$ (26), $CaCl_2$ (1), $MgCl_2$ (5), KCl (3), glucose (10), NaH_2PO_4 (1.25) plus $GABA_A$R antagonist bicuculline (10 μM) and NMDAR antagonist D-aminophosphonovalerate (APV, 25 μM). Patch pipettes (5–8 MΩ) were filled with internal solution containing (mM) Cs-methanesulfonate (130), CsCl (10), NaCl (4), $MgCl_2$ (1), HEPES (10), EGTA (5), QX-314 (2.2), phosphocreatine (12), MgATP (5), Na_2GTP (0.5), and leupeptin (0.1); pH 7.2–7.3, 265–270 mOsm. Neurons were observed with a ×40 water-immersion lens and illuminated with near infrared (IR) light, and the image was captured with an IR-sensitive CCD camera. Recordings were performed using a Multiclamp 700A amplifier (Axon Instruments). Tight seals (2–10 GΩ) were obtained by applying negative pressure. The membrane was ruptured with additional suction to obtain whole-cell configuration. Access resistance (13–18 MΩ) was compensated by 50–70%. Neurons were held at −70 mV. EPSCs were evoked by stimulating the neighbouring neurons (50 μs pulse) with a bipolar tungsten electrode (FHC, Inc.). To record mEPSC in PFC slices, slices were perfused with a modified ACSF containing a low concentration of $MgCl_2$ (1 mM) and TTX (1 μM). Data analysis was performed with Clampfit (Axon Instruments). Spontaneous synaptic events were analysed with Mini Analysis Program (Synaptosoft, Leonia, NJ). Statistical comparisons of the amplitude and frequency of mEPSC were made using the Kolmogorov–Smirnov test.

Supplementary data

Supplementary data are available at *The EMBO Journal* Online (http://www.embojournal.org).

Acknowledgements

This work was supported by the NIH grant NS046450 and NS035563 (JWH); NS035527 (RJW); MH-084233 (ZY); DA007339, DA016674, DA000513 (P-Y L); by Canadian Institutes for Health Research and the Michael Smith foundation for Health Research (MSFHR) (AEH), AEH was an MSFHR senior scholar; NIH training grant HL007121 (MAJ and DDH); an AHA award 0635357N (MAJ); and fellowships from the MSFHR and University Graduate Fellowship, UBC (MFL).

References

Banke TG, Bowie D, Lee H, Huganir RL, Schousboe A, Traynelis SF (2000) Control of GluR1 AMPA receptor function by cAMP-dependent protein kinase. *J Neurosci* **20:** 89–102

Berman DE, Dudai Y (2001) Memory extinction, learning anew, and learning the new: dissociations in the molecular machinery of learning in cortex. *Science (New York, NY)* **291:** 2417–2419

Burette A, Wyszynski M, Valtschanoff JG, Sheng M, Weinberg RJ (1999) Characterization of glutamate receptor interacting protein-immunopositive neurons in cerebellum and cerebral cortex of the albino rat. *J Comp Neurol* **411:** 601–612

Cahill L, Prins B, Weber M, McGaugh JL (1994) Beta-adrenergic activation and memory for emotional events. *Nature* **371:** 702–704

Chen L, Chetkovich DM, Petralia RS, Sweeney NT, Kawasaki Y, Wenthold RJ, Bredt DS, Nicoll RA (2000) Stargazing regulates synaptic targeting of AMPA receptors by two distinct mechanisms. *Nature* **408:** 936–943

Chen Y, Stevens B, Chang J, Milbrandt J, Barres BA, Hell JW (2008) NS21: re-defined and modified supplement B27 for neuronal cultures. *J Neurosci Methods* **171:** 239–247

Colledge M, Dean RA, Scott GK, Langeberg LK, Huganir RL, Scott JD (2000) Targeting of PKA to glutamate receptors through a MAGUK-AKAP complex. *Neuron* **27:** 107–119

Dahl D, Sarvey JM (1989) Norepinephrine induces pathway-specific long-lasting potentiation and depression in the hippocampal dentate gyrus. *Proc Natl Acad Sci USA* **86:** 4776–4780

Dai S, Hall DD, Hell JW (2009) Supramolecular assemblies and localized regulation of voltage-gated ion channels. *Physiol Rev* **89:** 411–452

Davare MA, Avdonin V, Hall DD, Peden EM, Burette A, Weinberg RJ, Horne MC, Hoshi T, Hell JW (2001) A beta2 adrenergic receptor signaling complex assembled with the Ca2+ channel Cav1.2. [see comments] [erratum appears in Science 2001 Aug 3;293:804]. *Science* **293:** 98–101

Davare MA, Dong F, Rubin CS, Hell JW (1999) The A-kinase anchor protein MAP2B and cAMP-dependent protein kinase are associated with class C L-type calcium channels in neurons. *J Biol Chem* **274:** 30280–30287

Davare MA, Hell JW (2003) Increased phosphorylation of the neuronal L-type Ca(2+) channel Ca(v)1.2 during aging. *Proc Natl Acad Sci USA* **100:** 16018–16023

Dingledine R, Borges K, Bowie D, Traynelis SF (1999) The glutamate receptor ion channel. *Pharmacol Rev* **51:** 7–61

Ehlers MD (2000) Reinsertion or degradation of AMPA receptors determined by activity-dependent endocytic sorting. *Neuron* **28:** 511–525

Esteban JA, Shi SH, Wilson C, Nuriya M, Huganir RL, Malinow R (2003) PKA phosphorylation of AMPA receptor subunits controls synaptic trafficking underlying plasticity. *Nat Neurosci* **6:** 136–143

Fischmeister R, Castro LR, Abi-Gerges A, Rochais F, Jurevicius J, Leroy J, Vandecasteele G (2006) Compartmentation of cyclic nucleotide signaling in the heart: the role of cyclic nucleotide phosphodiesterases. *Circ Res* **99:** 816–828

Gelinas JN, Nguyen PV (2005) Beta-adrenergic receptor activation facilitates induction of a protein synthesis-dependent late phase of long-term potentiation. *J Neurosci* **25:** 3294–3303

Gerrow K, Romorini S, Nabi SM, Colicos MA, Sala C, El-Husseini A (2006) A preformed complex of postsynaptic proteins is involved in excitatory synapse development. *Neuron* **49:** 547–562

Hall DD, Feekes JA, Arachchige Don AS, Shi M, Hamid J, Chen L, Strack S, Zamponi GW, Horne MC, Hell JW (2006) Binding of protein phosphatase 2A to the L-type calcium channel Cav1.2 next to Ser1928, its main PKA site, is critical for Ser1928 dephosphorylation. *Biochem* **45:** 3448–3459

Hollmann M, Heinemann S (1994) Cloned glutamate receptors. *Annu Rev Neurosci* **17:** 31–108

Hu XD, Huang Q, Yang X, Xia H (2007) Differential regulation of AMPA receptor trafficking by neurabin-targeted synaptic protein phosphatase-1 in synaptic transmission and long-term depression in hippocampus. *J Neurosci* **27:** 4674–4686

Katsuki H, Izumi Y, Zorumski CF (1997) Noradrenergic regulation of synaptic plasticity in the hippocampal CA1 region. *J Neurophysiol* **77:** 3013–3020

Leonard AS, Davare MA, Horne MC, Garner CC, Hell JW (1998) SAP97 is associated with the α-amino-3-hydroxy-5-methylisoxazole-4-propionic acid receptor GluR1 subunit. *J Biol Chem* **273:** 19518–19524

Leonard AS, Hell JW (1997) Cyclic AMP-dependent protein kinase and protein kinase C phosphorylate N-methyl-D-aspartate receptors at different sites. *J Biol Chem* **272:** 12107–12115

Leonard AS, Lim IA, Hemsworth DE, Horne MC, Hell JW (1999) Calcium/calmodulin-dependent protein kinase II is associated with the N-methyl-D-aspartate receptor. *Proc Natl Acad Sci USA* **96:** 3239–3244

Levitzki A (1988) From epinephrine to cyclic AMP. *Science* **241:** 800–806

Lim IA, Hall DD, Hell JW (2002) Selectivity and promiscuity of the first and second PDZ domains of PSD-95 and synapse-associated protein 102. *J Biol Chem* **277:** 21697–21711

Lim IA, Merrill MA, Chen Y, Hell JW (2003) Disruption of the NMDA receptor-PSD-95 interaction in hippocampal neurons with no obvious physiological short-term effect. *Neuropharmacology* **45:** 738–754

Lin YW, Min MY, Chiu TH, Yang HW (2003) Enhancement of associative long-term potentiation by activation of beta-adrenergic receptors at CA1 synapses in rat hippocampal slices. *J Neurosci* **23:** 4173–4181

Lise MF, Wong TP, Trinh A, Hines RM, Liu L, Kang R, Hines DJ, Lu J, Goldenring JR, Wang YT, El-Husseini A (2006) Involvement of myosin Vb in glutamate receptor trafficking. *J Biol Chem* **281:** 3669–3678

Lledo P-M, Zhang X, Sudhof TC, Malenka RC, Nicoll RA (1998) Postsynaptic membrane fusion and long-term potentiation. *Science* **279:** 399–403

Lu W, Man H, Ju W, Trimble WS, MacDonald JF, Wang YT (2001) Activation of synaptic NMDA receptors induces membrane insertion of new AMPA receptors and LTP in cultured hippocampal neurons. *Neuron* **29:** 243–254

Lu W, Shi Y, Jackson AC, Bjorgan K, During MJ, Sprengel R, Seeburg PH, Nicoll RA (2009) Subunit composition of synaptic AMPA receptors revealed by a single-cell genetic approach. *Neuron* **62:** 254–268

Lu Y, Allen M, Halt AR, Weisenhaus M, Dallapiazza RF, Hall DD, Usachev YM, McKnight GS, Hell JW (2007) Age-dependent requirement of AKAP150-anchored PKA and GluR2-lacking AMPA receptors in LTP. *EMBO J* **26:** 4879–4890

Man H-Y, Sekine-Aizawa Y, Huganir R (2007) Regulation of alpha-amino-3-hydroxy-5-methyl-4-isoxazolepropionic acid receptor trafficking through PKA phosphorylation of the Glu receptor 1 subunit. *Proc Natl Acad Sci USA* **104:** 3579–3584

Melone M, Burette A, Weinberg RJ (2005) Light microscopic identification and immunocytochemical characterization of glutamatergic synapses in brain sections. *J Comp Neurol* **492:** 495–509

Menuz K, Nicoll RA (2008) Loss of inhibitory neuron AMPA receptors contributes to ataxia and epilepsy in stargazer mice. *J Neurosci* **28:** 10599–10603

Menuz K, O'Brien JL, Karmizadegan S, Bredt DS, Nicoll RA (2008) TARP redundancy is critical for maintaining AMPA receptor function. *J Neurosci* **28:** 8740–8746

Minzenberg M, Watrous A, Yoon J, Ursu S, Carter C (2008) Modafinil shifts human locus coeruleus to low-tonic, high-phasic activity during functional MRI. *Science* **322:** 1700–1702

Neubig RR (1994) Membrane organization in G-protein mechanisms. *FASEB J* **8:** 939–946

Nielson KA, Jensen RA (1994) Beta-adrenergic receptor antagonist antihypertensive medications impair arousal-induced modulation of working memory in elderly humans. *Behav Neural Biol* **62:** 190–200

Oh MC, Derkach VA, Guire ES, Soderling TR (2006) Extrasynaptic membrane trafficking regulated by GluR1 Serine 845 phosphorylation primes AMPA receptors for long-term potentiation. *J Biol Chem* **281:** 752–758

Phend KD, Rustioni A, Weinberg RJ (1995) An osmium-free method of epon embedment that preserves both ultrastructure and antigenicity for post-embedding immunocytochemistry. *J Histochem Cytochem* **43:** 283–292

Phend KD, Weinberg RJ, Rustioni A (1992) Techniques to optimize post-embedding single and double staining for amino acid neurotransmitters. *J Histochem Cytochem* **40:** 1011–1020

Rebois RV, Hebert TE (2003) Protein complexes involved in heptahelical receptor-mediated signal transduction. *Receptors Channels* **9:** 169–194

Richter W, Day P, Agrawal R, Bruss MD, Granier S, Wang YL, Rasmussen SG, Horner K, Wang P, Lei T, Patterson AJ, Kobilka B, Conti M (2008) Signaling from beta1- and beta2-adrenergic receptors is defined by differential interactions with PDE4. *EMBO J* **27:** 384–393

Roche KW, O'Brien RJ, Mammen AL, Bernhardt J, Huganir RL (1996) Characterization of multiple phosphorylation sites on the AMPA receptor GluR1 subunit. *Neuron* **16:** 1179–1188

Sans N, Petralia RS, Wang YX, Blahos II J, Hell JW, Wenthold RJ (2000) A developmental change in NMDA receptor-associated proteins at hippocampal synapses. *J Neurosci* **20:** 1260–1271

Schiavo G, Matteoli M, Montecucco C (2000) Neurotoxins affecting neuroexocytosis. *Physiol Rev* **80:** 717–766

Schnell E, Sizemore M, Karimzadegan S, Chen L, Bredt DS, Nicoll RA (2002) Direct interactions between PSD-95 and stargazin control synaptic AMPA receptor number. *Proc Natl Acad Sci USA* **99:** 13902–13907

Seabold GK, Burette A, Lim IA, Weinberg RJ, Hell JW (2003) Interaction of the tyrosine kinase Pyk2 with the N-methyl-D-aspartate receptor complex via the src homology 3 domains of PSD-95 and SAP102. *J Biol Chem* **278:** 15040–15048

Seol GH, Ziburkus J, Huang S, Song L, Kim IT, Takamiya K, Huganir RL, Lee HK, Kirkwood A (2007) Neuromodulators control the polarity of spike-timing-dependent synaptic plasticity. *Neuron* **55:** 919–929

Sharif NA, Xu SX (2004) Binding affinities of ocular hypotensive beta-blockers levobetaxolol, levobunolol, and timolol at endogenous guinea pig beta-adrenoceptors. *J Ocul Pharmacol Ther* **20:** 93–99

Shenoy SK, Drake MT, Nelson CD, Houtz DA, Xiao K, Madabushi S, Reiter E, Premont RT, Lichtarge O, Lefkowitz RJ (2006) Beta-arrestin-dependent, G protein-independent ERK1/2 activation by the beta2 adrenergic receptor. *J Biol Chem* **281:** 1261–1273

Smith C, Teitler M (1999) Beta-blocker selectivity at cloned human beta 1- and beta 2-adrenergic receptors. *Cardiovasc Drugs Ther* **13:** 123–126

Strange BA, Dolan RJ (2004) Beta-adrenergic modulation of emotional memory-evoked human amygdala and hippocampal responses. *Proc Natl Acad Sci USA* **101:** 11454–11458

Strange BA, Hurlemann R, Dolan RJ (2003) An emotion-induced retrograde amnesia in humans is amygdala- and beta-adrenergic-dependent. *Proc Natl Acad Sci USA* **100:** 13626–13631

Sun X, Zhao Y, Wolf ME (2005) Dopamine receptor stimulation modulates AMPA receptor synaptic insertion in prefrontal cortex neurons. *J Neurosci* **25:** 7342–7351

Swayze RD, Lise MF, Levinson JN, Phillips A, El-Husseini A (2004) Modulation of dopamine mediated phosphorylation of AMPA receptors by PSD-95 and AKAP79/150. *Neuropharmacology* **47:** 764–778

Tavalin SJ, Colledge M, Hell JW, Langeberg LK, Huganir RL, Scott JD (2002) Regulation of GluR1 by the A-kinase anchoring protein 79 (AKAP79) signaling complex shares properties with long-term depression. *J Neurosci* **22:** 3044–3051

Thomas MJ, Moody TD, Makhinson M, O'Dell TJ (1996) Activity-dependent beta-adrenergic modulation of low frequency stimulation induced LTP in the hippocampal CA1 region. *Neuron* **17:** 475–482

Tomita S, Chen L, Kawasaki Y, Petralia RS, Wenthold RJ, Nicoll RA, Bredt DS (2003) Functional studies and distribution define a family of transmembrane AMPA receptor regulatory proteins. *J Cell Biol* **161:** 805–816

Valtschanoff JG, Burette A, Davare MA, Leonard AS, Hell JW, Weinberg RJ (2000) SAP97 concentrates at the postsynaptic density in cerebral cortex. *Eur J Neurosci* **12:** 3605–3614

Vanhoose AM, Winder DG (2003) NMDA and beta1-adrenergic receptors differentially signal phosphorylation of glutamate receptor type 1 in area CA1 of hippocampus. *J Neurosci* **23:** 5827–5834

Walling SG, Harley CW (2004) Locus ceruleus activation initiates delayed synaptic potentiation of perforant path input to the dentate gyrus in awake rats: a novel beta-adrenergic- and protein synthesis-dependent mammalian plasticity mechanism. *J Neurosci* **24:** 598–604

Wenthold RJ, Petralia RS, Blahos II J, Niedzielski AS (1996) Evidence for multiple AMPA receptor complexes in hippocampal CA1/CA2 neurons. *J Neurosci* **16:** 1982–1989

Winder DG, Martin KC, Muzzio IA, Rohrer D, Chruscinski A, Kobilka B, Kandel ER (1999) ERK plays a regulatory role in induction of LTP by theta frequency stimulation and its modulation by beta-adrenergic receptors. *Neuron* **24:** 715–726

Wu HY, Yuen EY, Lu YF, Matsushita M, Matsui H, Yan Z, Tomizawa K (2005) Regulation of N-methyl-D-aspartate receptors by calpain in cortical neurons. *J Biol Chem* **280:** 21588–21593

Xu J, Paquet M, Lau AG, Wood JD, Ross CA, Hall RA (2001) Beta 1-adrenergic receptor association with the synaptic scaffolding protein membrane-associated guanylate kinase inverted-2 (MAGI-2). Differential regulation of receptor internalization by MAGI-2 and PSD-95. *J Biol Chem* **276:** 41310–41317

Yuen EY, Gu Z, Yan Z (2007) Calpain regulation of AMPA receptor channels in cortical pyramidal neurons. *J Physiol* **580:** 241–254

Zaccolo M, Pozzan T (2002) Discrete microdomains with high concentration of cAMP in stimulated rat neonatal cardiac myocytes. *Science* **295:** 1711–1715

